

Lowering the Operating Temperature of Gold Acetylene Hydrochlorination Catalysts Using Oxidized Carbon Supports

Samuel Pattison,^{*,#} Simon R. Dawson,[#] Grazia Malta, Nicholas F. Dummer, Louise R. Smith, Anna Lazaridou, David J. Morgan, Simon J. Freakley, Simon A. Kondrat, Joost J. Smit, Peter Johnston, and Graham J. Hutchings^{*}



Cite This: *ACS Catal.* 2022, 12, 14086–14095



Read Online

ACCESS |



Metrics & More



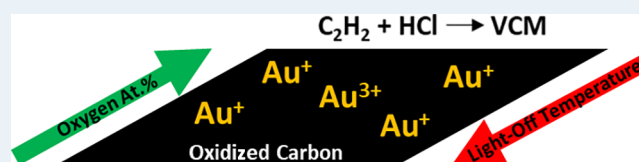
Article Recommendations



Supporting Information

ABSTRACT: The commercialization of gold for acetylene hydrochlorination represents a major scientific landmark. The development of second-generation gold catalysts continues with a focus on derivatives and drop-in replacements with higher activity and stability. Here, we show the influence that the support surface oxygen has on the activity of carbon supported gold catalysts. Variation in the surface oxygen content of carbon is achieved through careful modification of the Hummers chemical oxidation method prior to the deposition of gold. All oxidized carbon-based catalysts resulted in a marked increase in activity at 200 °C when compared to the standard nontreated carbon, with an optimum oxygen content of ca. 18 at % being observed. Increasing oxygen and relative concentration of C–O functionality yields catalysts with light-off temperatures 30–50 °C below the standard catalyst. This understanding opens a promising avenue to produce high activity acetylene hydrochlorination catalysts that can operate at lower temperatures.

KEYWORDS: gold, acetylene, hydrochlorination, vinyl chloride, light-off



INTRODUCTION

The replacement of mercuric chloride as a catalyst for vinyl chloride monomer (VCM) production from acetylene hydrochlorination has presented a major challenge in catalyst design. The signing of the Minamata convention generated much interest in this area and resulted in focused research efforts on developing a stable and environmentally friendly alternative.^{1,2} Despite the successful commercialization of gold catalysts for this reaction, the search continues for more effective catalysts. Various efforts to achieve this have focused on the formation of bimetallic catalysts incorporating gold with an additional metal,^{3–10} modification of the carbon support,¹¹ use of nonmetallic promoters,^{12,13} replacement of Au with alternative noble and non-noble metals,^{14–23} and removal of the metal altogether.^{24–27} Hutchings first predicted that gold would be the best catalyst for this reaction, which was later confirmed experimentally.^{28,29} Early gold catalysts were deemed not suitable for commercialization due to rapid deactivation caused by sintering of gold and coking. Johnston et al. later developed a stable gold catalyst by employing thiosulfate as a stabilizing ligand. Subsequent work has confirmed atomically dispersed gold as the active species and elucidated the role of sulfur and chloride ligands.^{30,31}

Recent research has focused attention on the nature of surface oxygenated groups (SOGs) on carbon supports as these can be shown to influence catalyst performance. Studies have shown that using aqua regia as a solvent for the gold precursor oxidizes both carbon and gold.³² Later, it was found

that oxidizing the carbon first using nitric acid prior to the deposition of the gold gave higher activity catalysts.³³ Using temperature programmed desorption coupled with mass spectroscopy enabled the SOGs to be probed and the increase in activity was correlated with the increase in phenol, ether, and carbonyl surface functionalities.

A similar nitric acid treatment of the support also yielded high activity gold catalysts.²² However, in this case, the oxidized materials were found to be far less stable. A correlation between high activity and low stability was suggested to be linked to the anchoring properties of the support, with all stable materials providing low activity. A green alternative to the aqua regia method, utilizing H₂O₂/HCl mixtures, was also found to modify the SOGs on the carbon support.³⁴ A higher proportion of SOGs such as carbonyl groups were found to improve the catalytic activity and stability of AuCl_x species through the formation of –O– linkages. A recent study by Pérez-Ramírez and co-workers has further elucidated the role of SOGs in the activity and stability of carbon supported Pt, Ru, and Au acetylene hydro-

Received: August 26, 2022

Revised: October 15, 2022

chlorination catalysts.³⁵ Analysis of a series of carbons with varying oxygen contents allowed the team to confirm that a higher content of acidic groups on the carbon surface leads to a higher degree of coking in Pt and Ru catalysts, dramatically increasing deactivation. Increased oxygen functionality was demonstrated to increase the activity of Ru and Au catalysts, albeit at the expense of stability, which is in good agreement with the work described above and previous literature investigating the effect of nitric acid treatments on Ru catalysts.³⁶ However, a minimum level of oxygen functionality was deemed to be necessary for Au catalysts to provide suitable anchoring sites for atomically dispersed species, with Au supported on highly reduced carbons resulting in nanoparticle formation.

Light-off temperature is a critical factor in applying gold-catalysts in existing industrial reactors. Any successful hydrochlorination catalyst will have to balance overall activity to prevent a high hotspot against a light-off temperature that allows starting up the catalyst within the available temperature range that the existing reactor has been designed for. Lowering the light-off temperature could result in catalysts that are able to start-up at lower temperatures while still not requiring excess gold that would increase the activity and result in excessive hot spots. Average axial temperature is a function of reactor tube diameter and intrinsic catalyst activity and determines the conversion and lifetime that can be achieved in a single tube length. Due to the exothermic nature of the reaction, the activity and tube diameter have a large effect on axial temperature distribution and on the hotspot, while the effect on conversion is relatively small.^{37,38}

In this work, we employed a modified Hummers technique³⁹ as a harsher method of oxidation of the carbon support to study the effect of significantly higher oxygen concentrations on the activity and stability of gold catalysts. Here we show that there is a direct correlation between the degree of oxidation of the carbon support and its catalytic activity when gold is added. Specific surface functionality, in the form of C–O, is demonstrated to be a key descriptor of low temperature activity, even when considering other literature catalysts.

EXPERIMENTAL SECTION

Chemicals. 5% Acetylene/argon (C₂H₂/Ar) (BOC, >95%), 5% hydrogen chloride/argon (HCl/Ar) (BOC, >95%), argon, (Air products, 99.9999%), hydrochloric acid (Fisher, 37%) nitric acid (Fisher, 70%), chloroauric acid (Alfa Aesar, 99.99%), activated carbon (AC) (Norit ROX 0.8), potassium permanganate (Sigma Aldrich, 97%), and hydrogen peroxide (Fluka, 30%) were all purchased and used without further purification.

Preparation of Standard 1% Au/C. In this study, a loading of 1 wt % Au was used despite the commercial catalyst operating using 0.1 wt % Au. A higher loading was used in the present study to aid the characterization of fresh and used materials.²⁹ Chloroauric acid (20 mg) was dissolved in aqua regia (3 HCl:1 HNO₃) (2.7 mL) and allowed to stir for 10 min. The metal precursor solution was added dropwise under stirring to ground, activated, dry carbon (0.99 g). This solution was left to stir for 1 h then dried under nitrogen at 140 °C for 16 h.

Preparation of Oxidized Carbons. Ground AC was oxidized according to a modified Hummers method.³⁹ AC (5 g) was treated with concentrated sulfuric (87.5 mL) and nitric acid (27.5 mL) with vigorous stirring and cooled (10 °C).

Potassium permanganate (0.5–10 g) was added stepwise over 2 h maintaining the mixture at <10 °C. The mixture was gradually warmed over 4 h to 20 °C, then heated (35 °C, 30 min). Deionized water (250 mL) was added, and the temperature rose to 70 °C. After 15 min, deionized water (1 L) was further added followed by hydrogen peroxide (3%) to quench any residual oxidant. The mixture was allowed to settle (16 h) after which the carbon was separated and washed repeatedly via centrifugation until a neutral pH was obtained and then dried (30 °C under vacuum, 16 h). Gold was then deposited on each of the oxidized carbons as described above.

Reaction Conditions for Acetylene Hydrochlorination. Unless otherwise stated, all reactions were conducted using the following conditions. The reactor was purged with Ar prior to the introduction of reactant gases. The reactor was then heated to and maintained at 200 °C for 30 min in flowing Ar (50 mL min⁻¹). C₂H₂/(5.01% in Ar, 23.56 mL min⁻¹), HCl (5.05% in Ar, 23.76 mL min⁻¹), and Ar (2.70 mL min⁻¹) were then introduced to the reactor which contained the catalyst (90 mg) giving a combined gas flow rate of 50 mL min⁻¹ (~17,600 h⁻¹ GHSV) and a C₂H₂:HCl ratio of 1:1.02 at ambient pressure. Full conversion and selectivity under these conditions would provide a VCM productivity of 35.33 mol kg_{cat}⁻¹ h⁻¹. Analysis of the acetylene hydrochlorination reaction was carried out using a Varian CP-3800 GC fitted with a Poropak-N packed column and a flame ionization detector. Conversion of acetylene was calculated using eq 1. In all tests, the VCM peak area closely correlated with the loss of acetylene, confirming that VCM was the only product.

$$\begin{aligned} \text{Acetylene conversion (\%)} \\ = \frac{\text{Initial acetylene peak area} - \text{Final acetylene peak area}}{\text{Initial acetylene peak area}} \\ \times 100 \end{aligned} \quad (1)$$

Deactivation rate was calculated according to eq 2.

$$\text{Deactivation rate (\%h}^{-1}\text{)} = \frac{X_{\text{MAX}} (\%) - X_{\text{RESIDUAL}} (\%)}{\Delta t (\text{h})} \quad (2)$$

where X_{MAX} = maximum C₂H₂ conversion, X_{RESIDUAL} = C₂H₂ conversion at steady state determined after the initial induction period,⁹ and Δt = time taken for conversion to decrease from maximum to the residual level.

Powder X-ray Diffraction. Analysis was performed between 10° and 80° 2 θ using an X'Pert Pro PAN Analytical powder diffractometer employing a Cu K α radiation source operating at 40 keV and 40 mA. Analysis of the spectra obtained was carried out using X'Pert High Score Plus software.

X-ray Photoelectron Spectroscopy. Analysis was performed on a Thermo Fisher Scientific K-alpha⁺ spectrometer. Data analysis was performed in CasaXPS using a Shirley type background and Scofield cross sections, with an energy dependence of -0.6.⁴⁰ Fitting was performed using the Lorentzian–Asymmetric (LA) and Finite LA (LF) lines shape in CasaXPS. These line shapes are based on a numerical convolution of a Lorentzian with a Gaussian to allow the production of both Voigt and asymmetric Voigt like line shapes. The specific parameters used were LA (1.53, 243) for Voigt like functions and LF (0.8, 1.2, 100, 100, 2) which have been derived from a large number of well-defined carbon

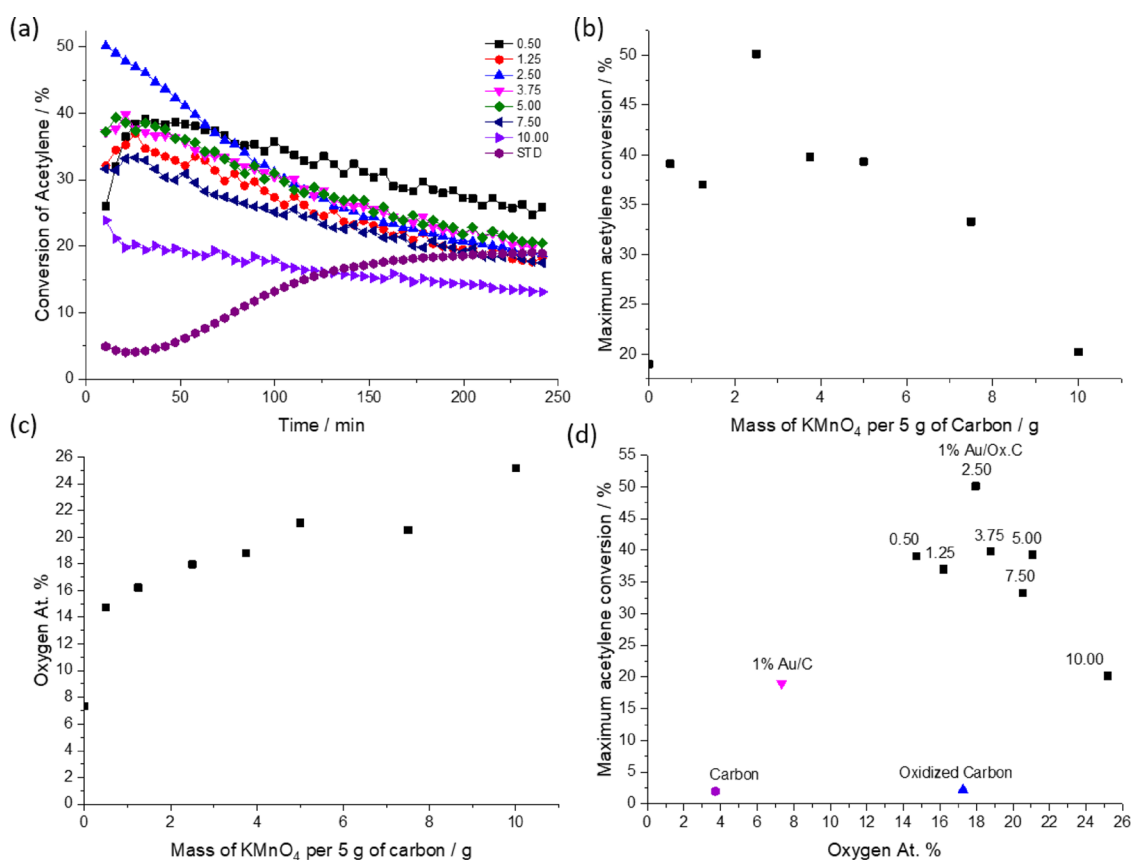


Figure 1. (a) Effect of time on line on acetylene conversion at 200 °C for Au catalysts supported on oxidized carbon treated with KMnO₄ (Xg/5 g carbon), where X = 0.50–10.00; 0.50 (black square), 1.25 (red circle), 2.50 (blue triangle), 3.75 (pink inverted triangle), 5.00 (green diamond), 7.50 (blue left arrow), 10.00 (violet right arrow) and Au/C standard (X = 0) (purple hexagon). (b) Maximum initial acetylene conversion (time on line 30 min) of oxidized carbon supported Au catalysts prepared with different masses of KMnO₄, (c) oxygen atomic % versus mass of KMnO₄ per 5 g of carbon. (d) Oxygen atomic percent of the oxidized carbon supported Au catalysts (black squares), Au/C standard (pink inverted triangle), oxidized (blue triangle), and unoxidized (purple hexagon) metal-free carbon versus maximum acetylene conversion.

samples such as highly oriented pyrolytic graphite and nanotubes.⁴¹ For fitting, the full-width half maximum of peaks (except for sp² carbon peak defined by the LF line shape) was considered to be equal. This resulted in the total concentrations of the fitted carbon–oxygen components to be within 1 at % of each other, the small discrepancy is attributed to both the asymmetric tail of the sp² carbon and the spectral background as discussed in the literature.⁴¹

X-ray Absorption Spectroscopy. X-ray absorption fine structure (XAFS) spectra were recorded at the B18 beamline of Diamond Light Source in Harwell, UK. Measurements were performed using a quick scanning extended XAFS setup with a fast-scanning Si (111) double crystal monochromator or a 36 element Ge fluorescence detector. Data were analyzed using Athena, from the Demeter software package.^{42,43} Samples were analyzed ex situ at the Au L₃ absorption edge in transmission mode. All analysis was performed with reference to an Au foil standard and KAuCl₄ and AuCl₂[−] standard compounds. Extended XAFS (EXAFS) fitting parameters are stated in the Supporting Information (Table S1). The relative amounts of each valence state were determined from the linear combination of standard spectra using the linear combination fitting (LCF) function in the Athena software.⁴⁴

N₂ Physisorption. A 3-Flex Micromeritics and a N₂ as gas adsorbent at 77 K was used for the surface analysis of the samples. Information about the micropore volume and the external surface outside the micropores was obtained by the

analysis of the *t*-plot. Micropore volume was obtained by extrapolating using the Harkins–Jura method.⁴⁵

RESULTS AND DISCUSSION

Optimization of Support Oxidation. Initially, a range of oxidized carbons were prepared using a modified Hummers method whereby the mass of KMnO₄ (0.50, 1.25, 2.50, 3.75, 5.00, 7.50, and 10.00 g) per 5 g of AC was varied in the preparation. Gold was then deposited on each of these oxidized carbon supports and the activity for acetylene hydrochlorination was compared at 200 °C. Each of the catalysts exhibit the same overall trend whereby high initial activity, after a brief induction period, is followed by a steady decline in conversion which continues for the duration of the experiment (Figure 1a). This decrease in conversion is associated with deactivation by the formation of gold nanoparticles, confirmed by X-ray diffraction (XRD) analysis of the fresh and used materials (Figure S1a,b), rather than each catalyst approaching a steady oxidation state of gold. Therefore, the maximum initial conversion (taken at 30 min of reaction) of each catalyst was plotted against the mass of KMnO₄ per 5 g of carbon (Figure 1b). Here, an optimum level of support oxidation is apparent whereby a maximum conversion is achieved using 2.50 g of oxidant per 5 g of carbon. Further increasing the level of oxidation has a detrimental effect on the activity of the final catalyst, with the lowest initial activity of the set achieved using 10 g of

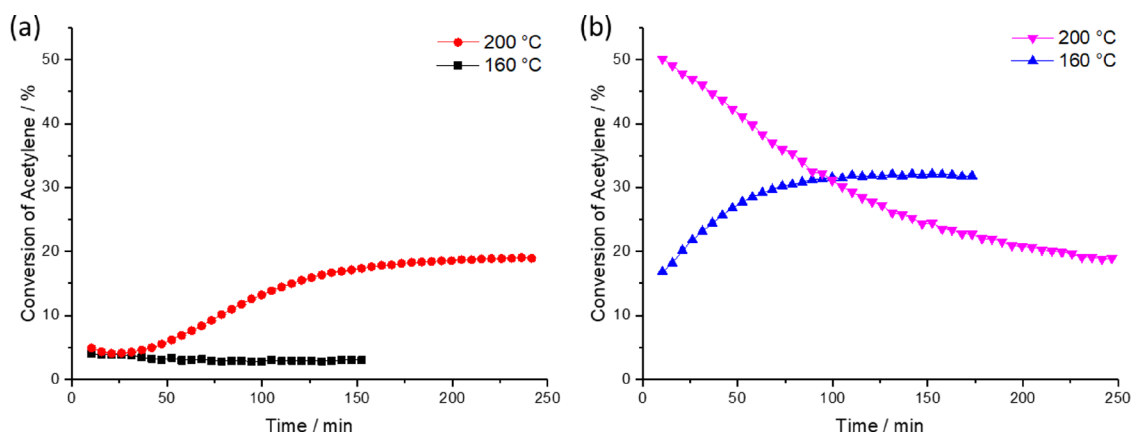


Figure 2. (a) Time-online acetylene conversion for 1% Au/C standard at 200 and 160 °C. (b) Time on-line study acetylene conversion for 1% Au/Ox C – 2.5 at 200, 160 °C.

KMnO₄ per 5 g of carbon. X-ray photoelectron spectroscopy (XPS) analysis of the range of oxidized carbon supported catalysts demonstrated that the trend in atomic percentage of oxygen (O at %) is nonlinear with respect to the amount of KMnO₄ used per 5 g of carbon (Figure 1c), a similar trend to that observed in our previous work.^{46,47} Therefore, the comparison of maximum activities as a function of O at % is more appropriate than the amount of oxidant used (Figure 1d). This clearly demonstrates the effect of oxidation of the support, with an optimum of ca. 18% being observed. The activity of the standard Au/C catalyst also appears to coincide with this trend. It should be noted that the oxidized carbon supports displayed low activity in the absence of Au, similar to the standard carbon, as shown using the support with the apparent optimum oxygen content (Figure 1d). This confirms that the observed increase in activity was not due to contribution from the support and rather due to the influence of oxygen on the active species. XPS analysis found no evidence of residual K or Mn from the KMnO₄ oxidant. ICP-MS analysis confirmed that <3 mg K and <1 mg Mn remained on the surface from the original 2.5 g KMnO₄ used per 5 g support. It should also be noted that this carbon displays a similar level of oxidation to the analogous catalyst after the deposition of Au via aqua regia (17 and 18 O at %, respectively, (Figure 1d, Tables S2 and S3)), highlighting the relative mildness of the aqua regia solvent compared the Hummers preparation. The same method of Au deposition was found to have a more significant effect on the standard carbon whereby O at % increased from 3.7 to 7.3%. In both the standard material and the optimum oxidized material, aqua regia deposition resulted in an increase in C=O and a loss in C–O functionality. Further interrogation of the C 1s and O 1s region of the XPS was conducted to identify whether a correlation was present between the observed trend in activity and functionality of the support. Due to the changes in functionality and level of oxidation of the carbon resulting from the aqua regia solvent, all XPS analysis was conducted post Au deposition. Analysis of the C 1s region (Figure S2a) demonstrated that sp² carbon decreases with increasing oxidation leading to a higher sp³ content, while species such as C–O and C=O steadily increased in relative concentration from 5 to 12% and 3 to 11%, respectively. Analysis of the O 1s region (Figure S2b) showed a similar increase in the relative concentration of the C–O functionality, in the form of phenol, carboxylate, or ether, from 45 to 55% while C=O increased

from 36% in the unoxidized material to between 40 and 42% for all oxidized carbon supported catalysts. The peaks in the range 535–540 eV are related to shake-up satellites arising from carbonyl functions, most likely attached to the aromatic structure of the graphitic carbon.⁴⁸ Despite higher activity clearly being linked to the oxidation of the support, none of the above changes in functionality can explain the trend observed in catalyst activity and why a proposed optimum level of ca. 18 O at % exists. Previous literature studies were also able to correlate the higher activity and stability of nitric acid treated materials with the concentration of phenol, ether, and carbonyl SOGs.³³ Phenol and carbonyl groups were also found to correlate well with activity when utilizing H₂O₂/HCl mixtures in place of aqua regia.³⁴ A similar volcano type trend in activity as observed here, but for Pt/C catalysts, has been described by Pérez-Ramírez and co-workers, which was ascribed to an optimal acetylene adsorption.³⁵ This was found to be influenced by the porous properties of the carbon and, to a lesser extent, surface oxygen concentrations. A trade-off in activity and stability was also found for carbon supported Au and Ru catalysts with increased SOGs leading to higher activity and lower stability catalysts. However, it should be noted that the range and total level of oxidation in the above study (2.7–7.2 O at %) is far lower than those in the present work (4.5–25.2 O at %). N₂ physisorption analysis on selected oxidized carbons suggests that higher oxidation results in a dramatic loss of surface area and microporosity which could explain the observed drop in activity above 18 O at % (Table S4).

Low Temperature Activity and Au Speciation. Despite the increased activity as a result of support oxidation, all catalysts demonstrated continued deactivation at 200 °C. Interestingly, the rate of deactivation closely correlates with maximum acetylene conversion, suggesting no apparent link with the loss of specific functionality of the carbon and catalyst stability (Figure S3). Due to the high deactivation rates at 200 °C, the catalyst with the optimum O at % was investigated at a lower temperature of 160 °C. The standard Au/C catalyst demonstrated stable activity at 200 °C, however, it showed only minimal activity at 160 °C (Figure 2a). Conversely, the oxidized carbon supported catalyst displays high activity even when tested at the lower temperature (Figure 2b). A conversion of ca. 30% was obtained, after an initial induction period, and remained stable for the duration of the experiment (ca. 180 min). Analysis of the normalized Au L3-edge X-ray absorption near edge structure (XANES) can give detailed

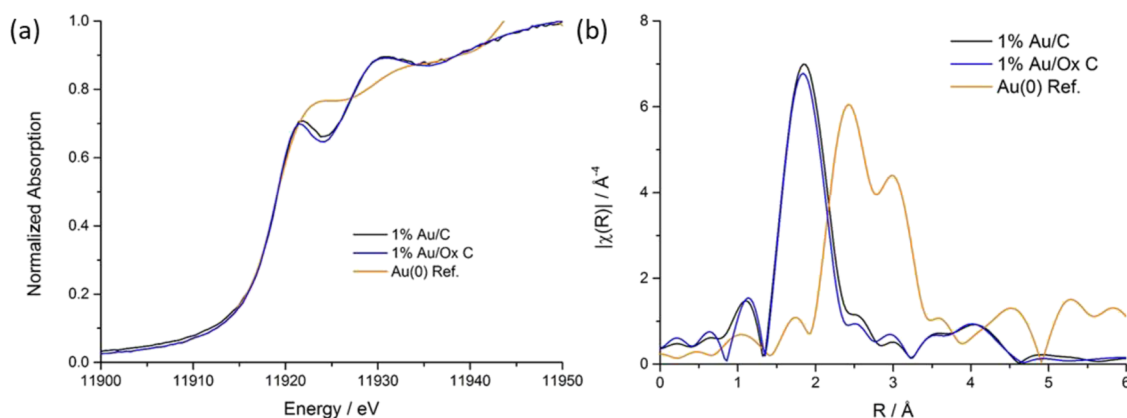


Figure 3. (a) Ex situ Au L_3 edge—normalized XANES spectra of 1% Au/C standard, 1% Au/Ox C – 2.5, and a gold-foil reference material. (b) k^3 – weighted χ EXAFS Fourier transform data of 1% Au/C standard, 1% Au/Ox C – 2.5, and a gold-foil reference material.

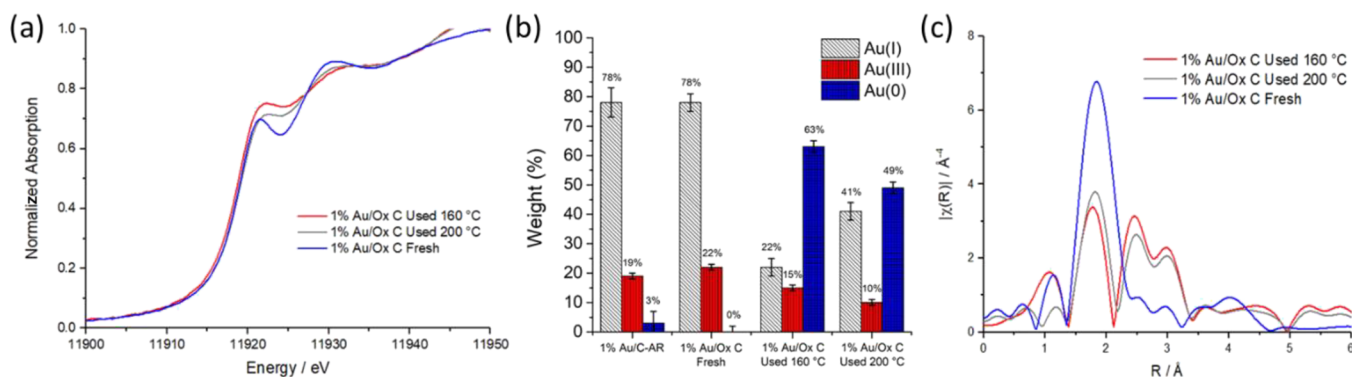


Figure 4. (a) Ex situ Au L_3 edge—normalized XANES spectra of 1% Au/Ox C – 2.5 fresh and the same catalyst used at 160 and 200 °C. (b) LCF of the Au L_3 -edge XANES for the fresh Au/C standard catalyst, and fresh and used at 160 and 200 °C 1% Au/Ox C – 2.5 catalysts. (c) k^3 – weighted χ EXAFS Fourier transform data of 1% Au/Ox C – 2.5 before and after use at 160 and 200 °C for 175 and 250 min, respectively.

information regarding Au speciation. Here, the strong absorption feature known as the white-line intensity represents Au $2p_{3/2}$ – $5d$ transitions, where higher Au oxidation states will lead to greater intensity in white-line height. Using appropriate standards, the Au oxidation state can be inferred.^{49,50} In our previous study, we demonstrated a strong correlation between white-line height and catalyst activity whereby highly active catalysts contained a high proportion of Au(I) but with a population of Au(III) also, indicating that a redox couple between the two states is crucial for high activity.³⁰ In the present study, ex situ XANES analysis of the standard 1% Au/C and optimized 1% Au/Ox C revealed little differences between the two samples, with both being predominantly comprised Au(I) (Figure 3a). This is demonstrated by the single peak at 11,920 eV with a normalized absorption of 0.7, with reference to Au(0). EXAFS analysis was unable to distinguish any major differences in Au–Cl speciation or indeed formation of Au–O between the fresh Au/C standard or oxidized carbon supported analogue (Figure 3b). Both samples display a single peak at 1.8 \AA relating to Au–Cl scattering and a double peak at 2.4 and 3.0 \AA , which signifies Au–Au, but can be considered negligible. The aqua regia preparation method has been previously shown to be efficient in the deposition of atomically dispersed Au, confirmed by high-angle annular dark-field scanning transmission electron microscopy and X-ray absorption spectroscopy (XAS) techniques.³⁰ The observed enhancement from support oxidation is therefore not considered to be due to an increase

in Au dispersion. Previous studies have shown that Au–O can be distinguished from Au–Cl in EXAFS with Au–O being represented by a peak at 0.3 \AA lower radial distance than Au–Cl.^{51–54} Here, no clear differences were observed, however this may be due to the high concentration of chloride (2–2.5 at %) in all samples and the weaker intensity of back-scattering from Au–OH.⁵¹ Despite the fresh catalysts having identical oxidation state and ligand environment, major differences were observed after being exposed to reaction conditions. After reaction at 200 °C, the oxidized carbon-supported Au catalyst undergoes significant reduction and formation of Au(0), demonstrated by a shallower absorption peak in XANES, similar to that of the Au(0) reference sample (Figure 4a). This is in good agreement with the post reaction XRD analysis (Figure S1b) and confirms the deactivation behavior during the reaction as being caused by sintering of the Au. Surprisingly, the sample tested at 160 °C appears to have formed Au(0) to a greater extent than when tested at 200 °C, despite the reaction profile appearing to stabilize over the reaction period. An LCF of the XANES results confirmed the similarity in Au(I), Au(III), and Au(0) ratios between fresh Au/C standard and Au/Ox C with 78:19:3 and 78:22:0, respectively (Figure 4b). Similar analysis of the Au/Ox C samples used at 200 and 160 °C confirmed a significant reduction of Au(I) and Au(III) to Au(0) with final proportions of 41:10:49 and 22:15:63, respectively. The level of Au reduction at 200 °C is expected, given the high initial conversion followed by the rapid deactivation and presence of

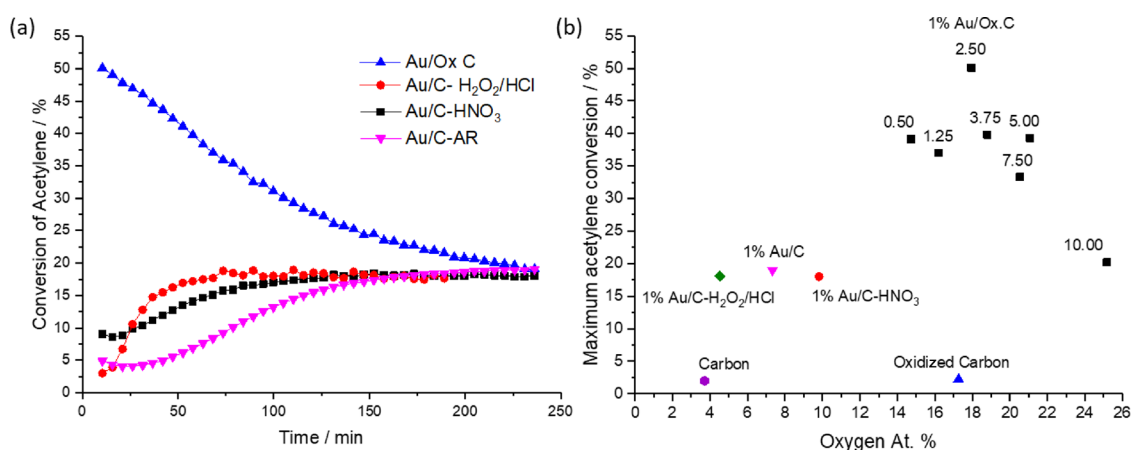


Figure 5. (a) Time-on-line acetylene conversion at 200 °C for Au/Ox C, Au/C–H₂O₂/HCl, Au/C–HNO₃, and Au/C standard. (b) Oxygen atomic percent of the oxidized carbon supported Au catalysts versus maximum acetylene conversion at 200 °C (black square). (Purple hexagon) denotes untreated carbon, (pink inverted triangle) 1% Au/C prepared with unoxidized carbon, (blue triangle) oxidized carbon prepared with 2.50 g of KMnO₄, (green diamond) Au/C–H₂O₂/HCl, and (red circle) Au/C–HNO₃.

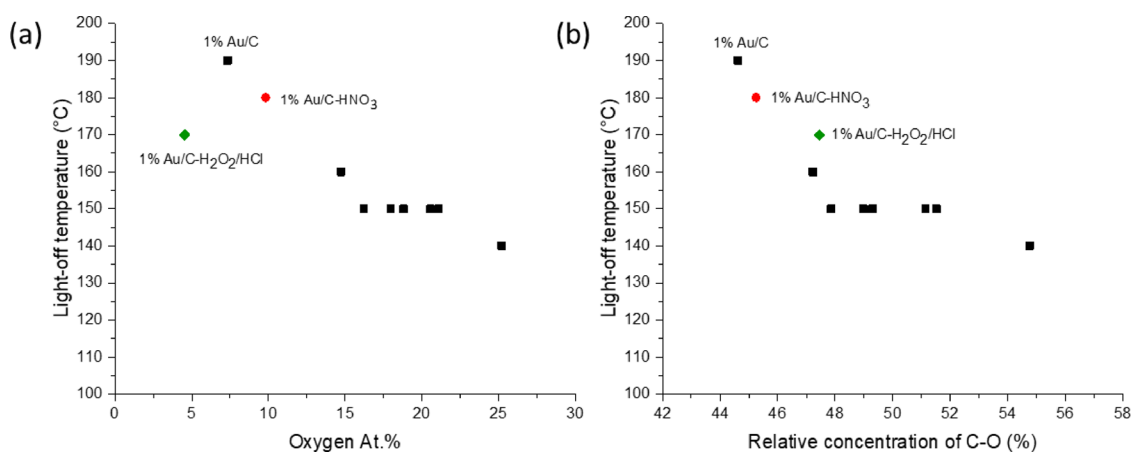


Figure 6. Comparison of light-off temperatures for Au/C–AR, oxidized carbon supported Au catalysts, Au/C–H₂O₂/HCl, and Au/C–HNO₃ against (a) oxygen at % and (b) relative concentration of C–O (%). (black squares) Aqua regia prepared unoxidized and oxidized carbon supported catalysts, (green diamond) Au/C–H₂O₂/HCl and (red circle) Au/C–HNO₃.

nanoparticles in XRD. This agrees with previous studies on 2% Au/C which found that the combination of high conversion and reaction conditions was favorable for the sintering of Au.⁵⁵ However, the increased reduction at a lower reaction temperature is perhaps surprising, given the high activity observed when compared to the standard Au/C, and seemingly stable reaction profile. Acetylene polymerization is known to occur at lower temperatures (below 100 °C), especially when employing acidic preparation methods or when gold is reduced to Au(0), however, in all tests the VCM produced correlated well with the expected level based on acetylene conversion.⁵⁶ It is likely that this catalyst would slowly deactivate over a longer reaction period at this temperature. The above changes in the oxidation state were partnered with changes in Au speciation by EXAFS (Figure 4c), where both the used 200 and 160 °C samples displayed a dramatic loss in Au–Cl and formation of a double peak at 2.4 and 3 Å representative of Au–Au scattering and Au(0) formation. It is clear then that oxidation of the support results in highly active catalysts but also significantly undermines catalyst stability, which agrees with previous literature on HNO₃ oxidized materials.²² The surface oxygen functionality was also found to differ between the fresh and used samples, with overall O at % decreasing from 18% in the

fresh sample to 16.4 and 15.5% in the 160 and 200 °C used samples, respectively (Tables S2 and S3). This loss is mainly associated with a loss in carbonyl functionality at 160 °C, with good agreement between O 1s and C 1s XPS regions. The relative concentration of oxygen groups appears to be similar in samples used at 160 and 200 °C suggesting the lower stability at higher temperature is not due to the further loss of functionality.

Comparison with Literature Catalysts. Previous studies have demonstrated that higher activity can be achieved by refluxing the carbon support in HNO₃ or by using oxidizing solvents such as H₂O₂/HCl.^{22,34} Preparation of these materials, following the reported procedures, confirmed that these are indeed much milder treatments than the Hummers oxidation of carbon used in this study. This resulted in a far lower level of oxidation of the support with H₂O₂/HCl and HNO₃ catalysts containing ca. 5 and 10 O at %, respectively, compared to the 18 O at % optimum oxidized carbon supported catalyst. The mildness of these methods is highlighted when considering the carbon support containing ca. 4 O at % prior to any treatment. Furthermore, only a minor effect on activity was observed when tested at 200 °C, mainly with respect to the induction period, with both Au/C–HNO₃ and Au/C–H₂O₂/HCl

reaching a similar final conversion to that of the standard Au/C prepared using aqua regia (Figure 5a). This is in stark contrast to the high initial activity observed using the optimum Hummers prepared material. The low level of oxidation and modest maximum conversion correlate well with our finding that a harsher oxidation of the support is required for high activity with an optimum of around 18 O at % (Figure 5b). The similarity in activities of Au/C–H₂O₂/HCl, Au/C standard, and Au/C–HNO₃ despite them having varying O at % (5, 7 and 10, respectively) may suggest that functionality plays a role rather than total at % of O. Alternatively, a minimum level of oxidation may be required for higher activity and materials below this will achieve largely similar conversions. It should also be noted that the literature tests were conducted at 180 °C, as opposed to 200 °C, and so the reported differences in activity when compared to the standard aqua regia material hint at an influence of functionalization on lower temperature VCM production.

Catalyst Light-off Temperature. In view of the enhanced low-temperature activity of the optimized Au/Ox C, these catalysts were further investigated to identify the light-off temperature, that is, the minimum temperature required to initiate the reaction above that of the blank reaction on the carbon support alone. This can be a key operating parameter in the commercial operation of these catalysts, and is particularly important in the replacement of Hg in existing reactors with specific operating temperature ranges. In each case, the catalyst was initially heated to 130 °C after which the sample was exposed to reaction gases and the temperature was periodically increased at 10 °C until acetylene conversion increased by $\geq 1\%$ /20 min. For the standard Au/C catalyst, light-off is achieved under the tested conditions at 190 °C (Figure S4). All oxidized carbons produced using the Hummers method resulted in a light-off temperature of 30–50 °C lower than that of the standard, with an apparent correlation between higher oxidized materials and lower light-off temperatures (Figure 6a). Au/C–HNO₃ and Au/C–H₂O₂/HCl both demonstrated a lower temperature light-off than the standard with 180 and 170 °C, respectively. This is despite these catalysts having a similar and lower level of at % O, respectively, compared to the standard. This could imply that the functionality of the carbon is important for lower temperature activity rather than overall at % O. Further analysis of the C 1s and O 1s XPS regions revealed that both samples correlate well with the previously observed trends for the oxidized carbons (Figure S5a,b), with the exception of C–O functionality in the Au/C–H₂O₂/HCl catalyst. This material appears to have an anomalously high level of C–O considering the overall level of oxidation. This material now correlates well with all other catalysts when considering the light-off temperature as a function of the relative concentration of C–O (Figure 6b). The nature of the influence of C–O on gold is unclear, with no obvious differences observed in any of the XAS performed in this study. Gold L₃-edge XANES analysis fresh Au/C–HNO₃ also demonstrated no obvious difference to the standard Au/C catalyst (Figure S6a). An LCF of the XANES confirmed that both are comprised of mainly Au(I) and a small contribution of Au(III) (Figure S6b). EXAFS analysis also demonstrated no difference in these samples with both displaying a single peak corresponding to Au–Cl, with no Au–Au scattering observed (Figure S6c). However, it is clear that the oxidation of the support, specifically through C–O functionalization, offers a key method for tuning the activity of gold catalysts.

CONCLUSIONS

The oxidation of the carbon support and its effect on the final activity of Au catalysts has been investigated for acetylene hydrochlorination. It was found that a range of oxygen atomic percent can be achieved using varying amounts of oxidant per 5 g of AC support. Each of these highly oxidized carbon-supported catalysts demonstrates an increased activity at 200 °C when compared to the standard Au/C material. An optimum level of oxidation of ca. 18 O at % is apparent after which further oxidation leads to lower activity catalysts due to dramatic reduction in the surface area and microporosity. The stability of these modified materials is low, with rapid deactivation being observed due to sintering of the gold and loss of the atomically dispersed active species. This agrees with previous literature which partnered increased oxidation with higher activity and lower stability catalysts through the investigation of milder treatments than that used in this study. In addition, each of these materials displayed a remarkable low temperature activity when compared to the Au/C standard with an apparent correlation between increasing O at % and lower light-off temperatures. C–O functionality, in the form of phenol, carboxylate, and ether, was found to be a key descriptor of low temperature activity with the relative concentration of C–O directly correlating with light-off temperatures, even when considering literature catalysts prepared by alternative oxidative treatments. At lower temperatures, the catalysts demonstrate a higher stability, however some formation of Au(0) is still observed via XAS analysis. This study highlights the influence of surface oxygen species and the tunability of the support and provides a basis for producing higher activity gold catalysts for acetylene hydrochlorination. In addition, this approach can be used to study the influence of surface oxidation for a number of applications which utilizes carbon as a catalyst support or as a metal-free carbocatalyst.

ASSOCIATED CONTENT

Supporting Information

The Supporting Information is available free of charge at <https://pubs.acs.org/doi/10.1021/acscatal.2c04242>.

Structural characterization of Au/C catalysts including XRD, XPS, XAS, and N₂ physisorption, plot of maximum acetylene conversion versus the deactivation rate of oxidized Au/C catalysts, deactivation rate and light-off temperature profiles, ex situ Au L₃ edge-normalized XANES spectra, LCF of the Au L₃-edge, EXAFS fitting parameters for Au L₃-Edge data for Au/C catalysts and standards, and comparison of relative concentrations of carbon 1s species for catalysts prepared with different oxygen atomic % (PDF)

AUTHOR INFORMATION

Corresponding Authors

Samuel Pattison – Max Planck Centre on the Fundamentals of Heterogeneous Catalysis FUNCAT, Cardiff Catalysis Institute, School of Chemistry, Cardiff University, Cardiff CF10 3AT, U.K.; Email: PattisonSD@cardiff.ac.uk

Graham J. Hutchings – Max Planck Centre on the Fundamentals of Heterogeneous Catalysis FUNCAT, Cardiff Catalysis Institute, School of Chemistry, Cardiff University, Cardiff CF10 3AT, U.K.; orcid.org/0000-0001-8885-1560; Email: Hutch@cf.ac.uk

Authors

Simon R. Dawson – Max Planck Centre on the Fundamentals of Heterogeneous Catalysis FUNCAT, Cardiff Catalysis Institute, School of Chemistry, Cardiff University, Cardiff CF10 3AT, U.K.

Grazia Malta – Max Planck Centre on the Fundamentals of Heterogeneous Catalysis FUNCAT, Cardiff Catalysis Institute, School of Chemistry, Cardiff University, Cardiff CF10 3AT, U.K.

Nicholas F. Dummer – Max Planck Centre on the Fundamentals of Heterogeneous Catalysis FUNCAT, Cardiff Catalysis Institute, School of Chemistry, Cardiff University, Cardiff CF10 3AT, U.K.; orcid.org/0000-0002-0946-6304

Louise R. Smith – Max Planck Centre on the Fundamentals of Heterogeneous Catalysis FUNCAT, Cardiff Catalysis Institute, School of Chemistry, Cardiff University, Cardiff CF10 3AT, U.K.

Anna Lazaridou – Max Planck Centre on the Fundamentals of Heterogeneous Catalysis FUNCAT, Cardiff Catalysis Institute, School of Chemistry, Cardiff University, Cardiff CF10 3AT, U.K.

David J. Morgan – Max Planck Centre on the Fundamentals of Heterogeneous Catalysis FUNCAT, Cardiff Catalysis Institute, School of Chemistry, Cardiff University, Cardiff CF10 3AT, U.K.; orcid.org/0000-0002-6571-5731

Simon J. Freakley – Department of Chemistry, University of Bath, Bath BA2 7AX, U.K.

Simon A. Kondrat – Department of Chemistry, Loughborough University, Loughborough LE11 3TU, U.K.; orcid.org/0000-0003-4972-693X

Joost J. Smit – Johnson Matthey, Catalyst Technologies, London W2 6LG, U.K.; orcid.org/0000-0002-9665-5997

Peter Johnston – Johnson Matthey, Catalyst Technologies, Billingham TS23 1LB, U.K.

Complete contact information is available at: <https://pubs.acs.org/10.1021/acscatal.2c04242>

Author Contributions

[#]S.P. and S.R.D. contributed equally to the experimental work.

Author Contributions

S.P., S.R.D., G.M., N.F.D., L.R.S., S.J.F., S.A.K., P.J., and G.J.H. contributed to the design of the study; S.P., S.R.D., and A.L. conducted experiments and data analysis; S.P., S.R.D., G.M., A.L., and D.J.M. conducted catalyst characterization and the corresponding data processing; S.P., S.R.D., J.J.S., P.J., and G.J.H. wrote the manuscript; S.P. and S.R.D. wrote the supplementary information. S.P., N.F.D., L.R.S., J.J.S., P.J., and G.J.H. commented on and edited both documents. All authors discussed and contributed to the work.

Notes

The authors declare no competing financial interest.

ACKNOWLEDGMENTS

The authors thank Johnson Matthey for funding. The authors also thank the Diamond Light Source for access to the B18 beamline for XAS studies (allocation numbers AP15214, SP15151-7, and SP15151-9).

REFERENCES

- (1) United Nations Environment Programme, Minamata Convention on Mercury www.mercuryconvention.org, (accessed January 10, 2022).
- (2) Liu, Y.; Zhao, L.; Zhang, Y.; Zhang, L.; Zan, X. Progress and Challenges of Mercury-Free Catalysis for Acetylene Hydrochlorination. *Catalysts* **2020**, *10*, 1218.
- (3) Zhang, H.; Dai, B.; Wang, X.; Li, W.; Han, Y.; Gu, J.; Zhang, J. Non-Mercury Catalytic Acetylene Hydrochlorination over Bimetallic Au–Co(III)/SAC Catalysts for Vinyl Chloride Monomer Production. *Green Chem.* **2013**, *15*, 829–836.
- (4) Zhang, H.; Li, W.; Li, X.; Zhao, W.; Gu, J.; Qi, X.; Dong, Y.; Dai, B.; Zhang, J. Non-Mercury Catalytic Acetylene Hydrochlorination over Bimetallic Au–Ba(II)/AC Catalysts. *Catal. Sci. Technol.* **2015**, *5*, 1870–1877.
- (5) Zhao, J.; Xu, J.; Xu, J.; Ni, J.; Zhang, T.; Xu, X.; Li, X. Activated-Carbon-Supported Gold-Cesium(I) as Highly Effective Catalysts for Hydrochlorination of Acetylene to Vinyl Chloride. *ChemPlusChem* **2015**, *80*, 196–201.
- (6) Pu, Y.; Zhang, J.; Wang, X.; Zhang, H.; Yu, L.; Dong, Y.; Li, W. Bimetallic Au–Ni/CSs Catalysts for Acetylene Hydrochlorination. *Catal. Sci. Technol.* **2014**, *4*, 4426–4432.
- (7) Zhao, J.; Gu, S.; Xu, X.; Zhang, T.; Di, X.; Pan, Z.; Li, X. Promotional Effect of Copper(II) on an Activated Carbon Supported Low Content Bimetallic Gold-Cesium(I) Catalyst in Acetylene Hydrochlorination. *RSC Adv.* **2015**, *5*, 101427–101436.
- (8) Zhang, H.; Dai, B.; Li, W.; Wang, X.; Zhang, J.; Zhu, M.; Gu, J. Non-Mercury Catalytic Acetylene Hydrochlorination over Spherical Activated-Carbon-Supported Au–Co(III)–Cu(II) Catalysts. *J. Catal.* **2014**, *316*, 141–148.
- (9) Dong, Y.; Zhang, H.; Li, W.; Sun, M.; Guo, C.; Zhang, J. Bimetallic Au–Sn/AC Catalysts for Acetylene Hydrochlorination. *J. Ind. Eng. Chem.* **2016**, *35*, 177–184.
- (10) Kaiser, S. K.; Clark, A. H.; Cartocci, L.; Krumeich, F.; Pérez-Ramírez, J. Sustainable Synthesis of Bimetallic Single Atom Gold-Based Catalysts with Enhanced Durability in Acetylene Hydrochlorination. *Small* **2021**, *17*, No. e2004599.
- (11) Dawson, S. R.; Pattison, S.; Malta, G.; Dummer, N. F.; Smith, L. R.; Lazaridou, A.; Allen, C. S.; Davies, T. E.; Freakley, S. J.; Kondrat, S. A.; Kiely, C. J.; Johnston, P.; Hutchings, G. J. Sulfur Promotion in Au/C Catalyzed Acetylene Hydrochlorination. *Small* **2021**, *17*, No. 2007221.
- (12) Zhang, C.; Zhang, H.; Li, Y.; Xu, L.; Li, J.; Li, L.; Cai, M.; Zhang, J. Hydrochlorination of Acetylene Over the Activated-Carbon-Supported Au Catalysts Modified by N–P–O-Containing Ligand. *ChemCatChem* **2019**, *11*, 3441–3450.
- (13) Li, Y.; Zhang, C.; Zhang, H.; Li, L.; Zhang, J.; Oh, R.; Yao, L.; Cai, M.; Li, J.; Zhang, M.; Li, F. Effects of N-, P-, or O-Containing Ligands on Gold-Based Complex Catalysts for Acetylene Hydrochlorination. *Appl. Catal., A* **2021**, *612*, No. 118015.
- (14) Kaiser, S. K.; Fako, E.; Manzocchi, G.; Krumeich, F.; Hauert, R.; Clark, A. H.; Safonova, O. V.; López, N.; Pérez-Ramírez, J. Nanostructuring Unlocks High Performance of Platinum Single-Atom Catalysts for Stable Vinyl Chloride Production. *Nat. Catal.* **2020**, *3*, 376–385.
- (15) Li, H.; Wu, B.; Wang, J.; Wang, F.; Zhang, X.; Wang, G.; Li, H. Efficient and Stable Ru(III)-Choline Chloride Catalyst System with Low Ru Content for Non-Mercury Acetylene Hydrochlorination. *Cuihua Xuebao/Chin. J. Catal.* **2018**, *39*, 1770–1781.
- (16) Li, X.; Zhang, H.; Man, B.; Zhang, C.; Dai, H.; Dai, B.; Zhang, J. Synthesis of Vinyl Chloride Monomer over Carbon-Supported Tris-(Triphenylphosphine) Ruthenium Dichloride Catalysts. *Catalysts* **2018**, *8*, 276.
- (17) Wang, X.; Lan, G.; Liu, H.; Zhu, Y.; Li, Y. Effect of Acidity and Ruthenium Species on Catalytic Performance of Ruthenium Catalysts for Acetylene Hydrochlorination. *Catal. Sci. Technol.* **2018**, *8*, 6143–6149.

- (18) Wang, L.; Wang, F.; Wang, J. Enhanced Stability of Hydrochlorination of Acetylene Using Polyaniline-Modified Pd/HY Catalysts. *Catal. Commun.* **2016**, *74*, 55–59.
- (19) Wang, L.; Wang, F.; Wang, J. Effect of K Promoter on the Stability of Pd/NFY Catalysts for Acetylene Hydrochlorination. *Catal. Commun.* **2016**, *83*, 9–13.
- (20) Zhai, Y.; Zhao, J.; Di, X.; Di, S.; Wang, B.; Yue, Y.; Sheng, G.; Lai, H.; Guo, L.; Wang, H.; Li, X. Carbon-Supported Perovskite-like CsCuCl₃ Nanoparticles: A Highly Active and Cost-Effective Heterogeneous Catalyst for the Hydrochlorination of Acetylene to Vinyl Chloride. *Catal. Sci. Technol.* **2018**, *8*, 2901–2908.
- (21) Zhao, W.; Zhu, M.; Dai, B. The Preparation of Cu-g-C₃N₄/AC Catalyst for Acetylene Hydrochlorination. *Catalysts* **2016**, *6*, 193–203.
- (22) O'Connell, K. C.; Monnier, J. R.; Regalbutto, J. R. The Curious Relationship of Sintering to Activity in Supported Gold Catalysts for the Hydrochlorination of Acetylene. *Appl. Catal., B* **2018**, *225*, 264–272.
- (23) Dai, H.; Zhu, M.; Zhang, H.; Yu, F.; Wang, C.; Dai, B. Activated Carbon Supported Mo-Ti-N Binary Transition Metal Nitride as Catalyst for Acetylene Hydrochlorination. *Catalysts* **2017**, *7*, 200.
- (24) Li, X.; Pan, X.; Bao, X. Nitrogen Doped Carbon Catalyzing Acetylene Conversion to Vinyl Chloride. *J. Energy Chem.* **2014**, *23*, 131–135.
- (25) Li, X.; Wang, Y.; Kang, L.; Zhu, M.; Dai, B. A Novel, Non-Metallic Graphitic Carbon Nitride Catalyst for Acetylene Hydrochlorination. *J. Catal.* **2014**, *311*, 288–294.
- (26) Wang, J.; Zhao, F.; Zhang, C.; Kang, L.; Zhu, M. A Novel S, N Dual Doped Carbon Catalyst for Acetylene Hydrochlorination. *Appl. Catal., A* **2018**, *549*, 68–75.
- (27) Li, P.; Li, H.; Pan, X.; Tie, K.; Cui, T.; Ding, M.; Bao, X. Catalytically Active Boron Nitride in Acetylene Hydrochlorination. *ACS Catal.* **2017**, *7*, 8572–8577.
- (28) Hutchings, G. J. Vapor Phase Hydrochlorination of Acetylene: Correlation of Catalytic Activity of Supported Metal Chloride Catalysts. *J. Catal.* **1985**, *96*, 292–295.
- (29) Johnston, P.; Carthey, N.; Hutchings, G. J. Discovery, Development, and Commercialization of Gold Catalysts for Acetylene Hydrochlorination. *J. Am. Chem. Soc.* **2015**, *137*, 14548–14557.
- (30) Malta, G.; Kondrat, S. A.; Freakley, S. J.; Davies, C. J.; Lu, L.; Dawson, S.; Thetford, A.; Gibson, E. K.; Morgan, D. J.; Jones, W.; Wells, P. P.; Johnston, P.; Catlow, C. R. A.; Kiely, C. J.; Hutchings, G. J. Identification of Single-Site Gold Catalysis in Acetylene Hydrochlorination. *Science* **2017**, *355*, 1399–1403.
- (31) Malta, G.; Kondrat, S. A.; Freakley, S. J.; Morgan, D. J.; Gibson, E. K.; Wells, P. P.; Aramini, M.; Gianolio, D.; Thompson, P. B. J.; Johnston, P.; Hutchings, G. J. In Situ K-Edge X-Ray Absorption Spectroscopy of the Ligand Environment of Single-Site Au/C Catalysts during Acetylene Hydrochlorination. *Chem. Sci.* **2020**, *11*, 7040–7052.
- (32) Conte, M.; Davies, C. J.; Morgan, D. J.; Davies, T. E.; Elias, D. J.; Carley, A. F.; Johnston, P.; Hutchings, G. J. Aqua Regia Activated Au/C Catalysts for the Hydrochlorination of Acetylene. *J. Catal.* **2013**, *297*, 128–136.
- (33) Xu, J.; Zhao, J.; Xu, J.; Zhang, T.; Li, X.; Di, X.; Ni, J.; Wang, J.; Cen, J. Influence of Surface Chemistry of Activated Carbon on the Activity of Gold/Activated Carbon Catalyst in Acetylene Hydrochlorination. *Ind. Eng. Chem. Res.* **2014**, *53*, 14272–14281.
- (34) Zhao, J.; Wang, B.; Yue, Y.; Di, S.; Zhai, Y.; He, H.; Sheng, G.; Lai, H.; Zhu, Y.; Guo, L.; Li, X. Towards a Greener Approach for the Preparation of Highly Active Gold/Carbon Catalyst for the Hydrochlorination of Ethyne. *J. Catal.* **2018**, *365*, 153–162.
- (35) Kaiser, S. K.; Surin, I.; Amorós-Pérez, A.; Büchele, S.; Krumeich, F.; Clark, A. H.; Román-Martínez, M. C.; Lillo-Ródenas, M. A.; Pérez-Ramírez, J. Design of Carbon Supports for Metal-Catalyzed Acetylene Hydrochlorination. *Nat. Commun.* **2021**, *12*, 4016.
- (36) Man, B.; Zhang, H.; Zhang, J.; Li, X.; Xu, N.; Dai, H.; Zhu, M.; Dai, B. Oxidation Modification of Ru-Based Catalyst for Acetylene Hydrochlorination. *RSC Adv.* **2017**, *7*, 23742–23750.
- (37) Chen, J.; Cheng, D. G.; Chen, F. Q. Simulation and Analysis of Fixed-Bed Reactor for Hydrochlorination of Acetylene. *Zhejiang Daxue Xuebao (Gongxue Ban)/J. Zhejiang Univ. Eng. Sci.* **2012**, *46*, 749–755.
- (38) Xu, H.; Luo, G. Green Production of PVC from Laboratory to Industrialization: State-of-the-Art Review of Heterogeneous Non-Mercury Catalysts for Acetylene Hydrochlorination. *J. Ind. Eng. Chem.* **2018**, *65*, 13–25.
- (39) Hummers, W. S.; Offeman, R. E. Preparation of Graphitic Oxide. *J. Am. Chem. Soc.* **1958**, *80*, 1339.
- (40) Fairley, N.; Fernandez, V.; Richard-Plouet, M.; Guillot-Deudon, C.; Walton, J.; Smith, E.; Flahaut, D.; Greiner, M.; Biesinger, M.; Tougaard, S.; Morgan, D.; Baltrusaitis, J. Systematic and Collaborative Approach to Problem Solving Using X-Ray Photoelectron Spectroscopy. *Appl. Surf. Sci. Adv.* **2021**, *5*, No. 100112.
- (41) Morgan, D. J. Comments on the XPS Analysis of Carbon Materials. *C* **2021**, *7*, 51.
- (42) Ravel, B.; Newville, M. ATHENA, ARTEMIS, HEPHAESTUS: Data Analysis for X-Ray Absorption Spectroscopy Using IFEFFIT. *J. Synchrotron Radiat.* **2005**, *12*, 537–541.
- (43) Newville, M. IFEFFIT: Interactive XAFS Analysis and FEFF Fitting. *J. Synchrotron Radiat.* **2001**, *8*, 322–324.
- (44) Lengke, M. F.; Ravel, B.; Fleet, M. E.; Wanger, G.; Gordon, R. A.; Southam, G. Mechanisms of Gold Bioaccumulation by Filamentous Cyanobacteria from Gold(III)-Chloride Complex. *Environ. Sci. Technol.* **2006**, *40*, 6304–6309.
- (45) Galarneau, A.; Villemot, F.; Rodriguez, J.; Fajula, F.; Coasne, B. Validity of the T-Plot Method to Assess Microporosity in Hierarchical Micro/Mesoporous Materials. *Langmuir* **2014**, *30*, 13266–13274.
- (46) Pattison, S.; Nowicka, E.; Gupta, U. N.; Shaw, G.; Jenkins, R. L.; Morgan, D. J.; Knight, D. W.; Hutchings, G. J. Tuning Graphitic Oxide for Initiator- and Metal-Free Aerobic Epoxidation of Linear Alkenes. *Nat. Commun.* **2016**, *7*, 12855.
- (47) Pattison, S.; Rogers, O.; Whiston, K.; Taylor, S. H.; Hutchings, G. J. Low Temperature Solvent-Free Allylic Oxidation of Cyclohexene Using Graphitic Oxide Catalysts. *Catal. Today* **2020**, *357*, 3–7.
- (48) Beamson, G.; Briggs, D. High Resolution XPS of Organic Polymers: The Scienta ESCA300 Database. *J. Chem. Educ.* **1993**, *70*, A25.
- (49) Chang, S. Y.; Uehara, A.; Booth, S. G.; Ignatyev, K.; Mosselmans, J. F. W.; Dryfe, R. A. W.; Schroeder, S. L. M. Structure and Bonding in Au(I) Chloride Species: A Critical Examination of X-Ray Absorption Spectroscopy (XAS) Data. *RSC Adv.* **2015**, *5*, 6912–6918.
- (50) Pantelouris, A.; Küper, G.; Hormes, J.; Feldmann, C.; Jansen, M. Anionic Gold in Cs₃AuO and Rb₃AuO Established by X-Ray Absorption Spectroscopy. *J. Am. Chem. Soc.* **1995**, *117*, 11749–11753.
- (51) Uehara, A.; Chang, S. Y.; Booth, S. G.; Schroeder, S. L. M.; Mosselmans, J. F. W.; Dryfe, R. A. W. Redox and Ligand Exchange during the Reaction of Tetrachloroaurate with Hexacyanoferrate(II) at a Liquid-Liquid Interface: Voltammetry and X-Ray Absorption Fine-Structure Studies. *Electrochim. Acta* **2016**, *190*, 997–1006.
- (52) Paclawski, K.; Zajac, D. A.; Borowiec, M.; Kapusta, C.; Fitzer, K. EXAFS Studies on the Reaction of Gold (III) Chloride Complex Ions with Sodium Hydroxide and Glucose. *J. Phys. Chem. A* **2010**, *114*, 11943–11947.
- (53) Chen, X.; Chu, W.; Chen, D.; Wu, Z.; Marcelli, A.; Wu, Z. Correlation between Local Structure and Molar Ratio of Au (III) Complexes in Aqueous Solution: An XAS Investigation. *Chem. Geol.* **2009**, *268*, 74–80.
- (54) Song, Z.; Kenney, J. P. L.; Fein, J. B.; Bunker, B. A. An X-Ray Absorption Fine Structure Study of Au Adsorbed onto the Non-Metabolizing Cells of Two Soil Bacterial Species. *Geochim. Cosmochim. Acta* **2012**, *86*, 103–117.
- (55) Malta, G.; Kondrat, S. A.; Freakley, S. J.; Davies, C. J.; Dawson, S.; Liu, X.; Lu, L.; Dymkowski, K.; Fernandez-Alonso, F.;

Mukhopadhyay, S.; Gibson, E. K.; Wells, P. P.; Parker, S. F.; Kiely, C. J.; Hutchings, G. J. Deactivation of a Single-Site Gold-on-Carbon Acetylene Hydrochlorination Catalyst: An X-Ray Absorption and Inelastic Neutron Scattering Study. *ACS Catal.* **2018**, *8*, 8493–8505.

(56) Nkosi, B.; Coville, N. J.; Hutchings, G. J.; Adams, M. D.; Friedl, J.; Wagner, F. E. Hydrochlorination of Acetylene Using Gold Catalysts: A Study of Catalyst Deactivation. *J. Catal.* **1991**, *128*, 366–377.